Investigating simulated coupling measurements for the FCC-ee

Student: Felicia Houng Teen Teen
Supervisor: Jacqueline Keintzel

9th June 2025 - 1st August 2025

1 The Path from the LHC to the HL-LHC and the Future Circular Collider.

The landscape of particle physics is markedly developed with the operation of the Large Hadron Collider (LHC) [1], hosted by the European Organization for Nuclear Research (CERN). With a circumference of 27 km, this collider lead to the discovery of the Higgs boson [2] in 2012, which won both Professors Francois Englert and Peter Higgs the 2013 Physics Nobel Prize. The LHC is designed to provide proton–proton collisions with a centre-of-mass energy of 14 TeV [3]. To extend the capabilities of the LHC, CERN is upgrading the accelerator to the High-Luminosity LHC (HL-LHC) [4]. The HL-LHC is scheduled for operation in 2029, aiming to increase instantaneous luminosities by a factor of 5 to 7.5 with respect to the nominal value of the LHC. The increased luminosity indicates the production of more data, allowing the detailed study of the known physics and potentially the new physics.

To explore even higher-energy frontiers, a new machine that can reach energies far beyond what the LHC can achieve is needed. CERN is currently studying the design of a $\sim$ 91 km successor to the LHC called the Future Circular Collider (FCC) [5]. The FCC is anticipated to occur in two phases, each targeting different physics goals. The FCC-ee [6] for electron-positron collision, responsible for precision measurements will start operate in the late 2040s and is expected to run for 15 years. Meanwhile, the FCC-hh that performs proton-proton collisions will reuse the existing infrastructure of the FCC-ee.

The large circumference and high energies of the FCC-ee require sophisticated correction systems to maintain beam quality throughout the accelerator ring. The two critical correction systems that form the foundation of beam optics control are the Global Hybrid Corrections (GHC) [7] and the Local Chromaticity Corrections (LCC) [8]. These correction schemes need to be designed to ensure stable beam operation and optimal luminosity performance.

2 Key Concepts Simplified

When a charged particle (q), moving at velocity ($\overrightarrow{v}$) is subjected to an electromagnetic field (EM), the Lorentz force experienced by the charged particle is:

$$\overrightarrow{F} = q(\overrightarrow{E} + \overrightarrow{v} \times \overrightarrow{B}) \tag{1}$$

where $\overrightarrow{B}$ is the magnetic field and $\overrightarrow{E}$ is the electric field. The longitudinal component of the electric field $E_{\parallel}$ is responsible for particle acceleration with $E_{\parallel} \parallel v_{\parallel}$. Meanwhile for the transverse direction, the magnetic field ($B_{\perp} \perp v_{\perp}$) deflects the particle without changing the absolute value of the particle's velocity $|\overrightarrow{v}|$. These pure transverse fields will lead to a circular orbit with bending radius ρ for which the Lorentz force has to equal the centripetal force:

$$q(E_{\perp} + vB_{\perp}) = m\frac{v^2}{\rho} \tag{2}$$

where $m = \gamma m_0$ is the relativistic mass of a particle with rest mass m_0. Since the electron is moving with velocity near to the speed of light (c), the effect of the magnetic field dominates the electric field. That is to say, the bending force is easier to be generated by a magnetic field in comparison to the electric field. Thus, only the transverse magnetic field is responsible for the bending and focusing of the beam in a high-energy accelerator. The momentum of the particle is:

$$p = mv,$$

then equation 2 can be written as:

$$p = qB\rho, \tag{3}$$

where $B\rho = \frac{p}{q}$ is known as magnetic rigidity [9] or magnetic stiffness, a measure of the resistance of a particle to deflection by magnetic fields. Here, ρ represents the radius of curvature of the particle's path when moving perpendicular to the magnetic field. The magnetic rigidity basically means how difficult it is to deflect a charged particle using a magnetic field. The higher the magnetic rigidity, the greater the resistance to deflection. Two particles follow the same trajectory through a magnetic field if they have the same rigidity, even if they have different masses and charges.

Since particles are stored in a storage ring, it has to undergo bending to ensure that it follows the designed orbit. The primary components responsible for bending particle trajectories is the dipole mangnet [10]. They generate a uniform magnetic field perpendicular to the beam direction, causing charged particles to travel along a curved path.

While dipoles control the beam direction, quadrupole magnets [11] provide transverse focusing. A quadrupole field varies linearly with displacement from the center, exerting a restoring force in one plane (focusing) and a defocusing force in the orthogonal plane. This alternating focusing and defocusing effect is crucial for beam stability, as it prevents particles from diverging uncontrollably. The focusing strength k of a quadrupole is defined

$$k = \frac{(e \cdot g)}{p} \tag{4}$$

where g is the magnetic field gradient. To ensure beam quality and stability, focusing (F) and defocusing (D) quadrupoles are arranged periodically with drift spaces (O) in between [12]. This configuration, known as a FODO lattice, provides net focusing in both transverse planes despite the alternating focusing nature of the individual quadrupoles.

The stability of the beam in a FODO lattice is analyzed using the transfer matrix formalism, where the phase advance [13] per cell μ determines the beam's behavior. The $\beta(s)$ varies periodically along the lattice, reaching its maximum at the focusing quadrupole (where the beam is widest) and its minimum at the defocusing quadrupole (where the beam is narrowest). The phase advance per cell must satisfy $0 < \mu < \pi$ to ensure stability. The FODO lattice exemplifies how alternating focusing and defocusing elements can maintain beam confinement over many turns.

As particles travel around the accelerator, they oscillate transversely. This is known as betatron oscillation [14]. In an ideal scenario, the motion in the horizontal (x) and vertical (y) planes are independent. However, imperfection such as skewed quadrupole field causes these motions to become coupled. This coupling essentially tilts the beam. To measure the position of beam and diagnose such effects, Beam Position Monitors (BPM)s [14] are used. The BPMs are placed in the quadrupole around the ring. If there is coupling, the BPMs will detect correlated signals in the x and y planes.

The BPMs deliver the center of mass of the beam. The signal generated by the electromagnetic field of the beam beam is described using the transfer impedance concept. The basic idea is that, when a charged particle passes through a BPM, it induces electrical signals in nearby electrodes. The horizontal (x) and vertical (y) positions of the beam are calculated by comparing these signals.

The data obtained from the BPMs is called turn-by-turn (TbT) data, that is a record of the x and y positions of the beam at each BPM for every single turn it makes around the ring. The BPMs work by having four metallic buttons around the beam pipe. The closer the beam is to a button, the stronger the electrical signal it induces. Fast electronics then digitize these signals every turn, giving us the position data. The data is analysed via Fourier analysis following by other measurements.

The number of transverse oscillations a particle makes per turn around an accelerator is known as tune Q [15]. The Q value must be carefully controlled to avoid resonances that can lead to beam loss or emittance growth. Typically, integer ($Q = n$) and half-integer ($2Q = n$) resonances are avoided. The tune is determined by the magnetic lattice and can be adjusted by changing the k value.

The beta function ($\beta(s)$) [16] is a parameter that describes the size and shape of the beam envelope resulting from the betatron oscillations. A location with a small $\beta(s)$ value indicates a tightly focused beam while a larger $\beta(s)$ value corresponds to a larger beam size. Ideally, the $\beta(s)$ is a smoot and periodic property determined by the magnetic lattice design. However, in reality, imperfection such as quadrupole misalignments causes cause deviations in the beta function, that is known as the beta beating ($\Delta\beta/\beta$) [16]. These deviations are undesirable and beam optics are actively corrected to keep the measured beta function as close as possible to the design.

Coupling [17] refers to the interaction between horizontal and vertical betatron oscillations, where perturbations in one plane influence motion in the other, often due to skew quadrupole fields or misalignments. The coupling coefficient $C = \frac{|<k_1>|}{|Q_x - Q_y|}$ quantifies this effect. Here, Q_x and Q_y represent the tune in x and y directions, respectively. Strong coupling can lead to emittance sharing between planes, thus reducing beam quality.

The phase advance describes how the betatron phase evolves between two points as it travels from one point in the accelerator to another. Proper phase advance control ensures matched optics and minimizes resonance-driven instabilities.

3 Project here at CERN

The main goal of this 8-weeks project was to perform coupling modeling in the FCC-ee by looking at both the TbT (fixed at 1000 turns) optics measurement of LCC and GHC schemes. This was done in four main steps. First, the TbT data is simulated udder ideal conditions before introducing linear coupling into the simulation. This step is achieved by introducing skew quadrupole components onto all regular quadrupoles where the strength of these components is randomly distributed with a standard deviation of 10×10^{-6}. The distribution is truncated at $\pm\sigma$. Parameter scan was performed by varying the BPM resolution (BPM noise) and the initial kick strength given to the beam. Finally, the plots for coupling and phase advance were plotted using the TbT data.

To achieve this goal, several activities were undertaken. A foundational understanding of accelerator physics and beam dynamics was gained through reading. The Xsuite [18] simulation software was installed and used. Work was started with a simple FODO cell example to become familiar with the tools. The different FCC designs, specifically LCC and GHC were then studied. Using Xsuite, the optics parameters for the FCC were calculated. The OMC3 tool [19] was also utilized for the analysis of the TbT data and the effects of different simulation parameters were explored.

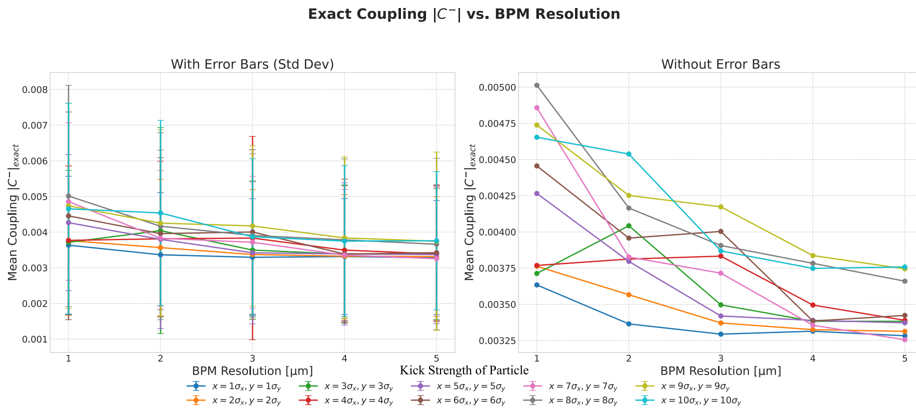

Figure 1: Plot of the BPM resolution against the exact mean coupling value across 51 error seeds with error bars (left) and without error bars (right) of the GHC.

4 Results and discussion

Figure 1 shows the plot of the BPM resolution against the exact mean coupling value across 51 error seeds with (left) and without error bars (right) of the GHC. The error bars of the GHC coupling plot fall in a reasonable range with a maximum accuracy of ~ 0.002 (see Fig. 1 (left)). In Fig. 1 (right), with the removal of error bars, it is shown that for $x = X\sigma_x$ and $y = X\sigma_y$, where $X = 1, 2, 3, ...$, the kick strengths of both σ_x and $\sigma_y \geq 2$ are quite stable.

Following by the coupling plot, the mean value of the phase advance plot is analysed. However, the error bar of ~ 0.3 appears inconsistent with expectations and requires further verification. Therefore, the corresponding plot is omitted pending additional investigation.

Figure 2 shows the plot of the BPM resolution against the exact mean coupling value across 51 error seeds with error bars (left) and without error bars (right) of the LCC. Although the order of magnitude of the error bars for LCC looks reasonable, the decrease of mean coupling values with the increase of BPM resolution is unusual.

5 Conclusion and outlook

In conclusion, the TbT measurements for both GHC and LCC optics have been simulated. The coupling was evaluated by varying several parameters, including the number of seeds, BPM resolutions and kick strengths. It was found that a larger kick in the x-direction has a more significant effect than a larger kick in the y-direction due to the larger beam size in the x-plane.

Looking ahead, further studies are needed for the LCC optics to understand the puzzling results that were observed. Besides, the phase advance measure-

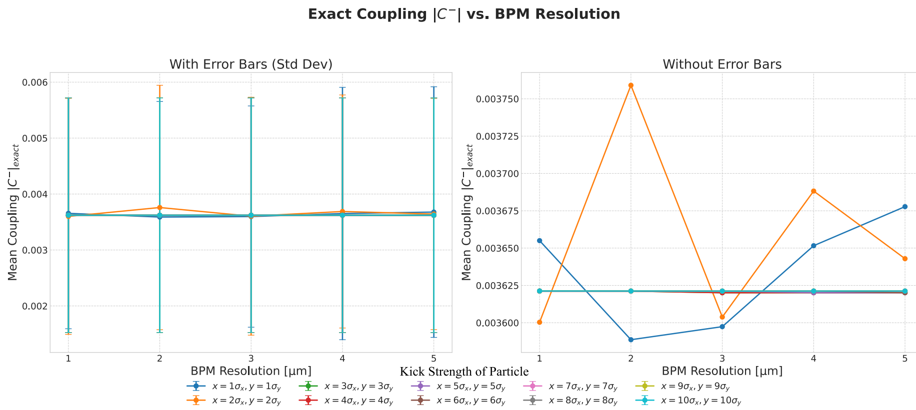

Figure 2: Plot of the BPM resolution against the exact mean coupling value across 51 error seeds with error bars (left) and without error bars (right). of the LCC.

ments need to be investigated further. A scan through a different number of turns and an exploration of measurements for an AC dipole are also forseen.

References

[1] Lyndon Evans. The large hadron collider. *Annual review of nuclear and particle science*, 61(1):435–466, 2011.

[2] George Watson and Peter Higgs. What is a boson? 1998.

[3] Lyndon Evans and Philip Bryant. Lhc machine. *Journal of instrumentation*, 3(08):S08001, 2008.

[4] Giorgio Apollinari, I Béjar Alonso, Oliver Brüning, M Lamont, and Lucio Rossi. High-luminosity large hadron collider (hl-lhc): Preliminary design report. Technical report, Fermi National Accelerator Lab.(FNAL), Batavia, IL (United States), 2015.

[5] Michael Benedikt and Frank Zimmermann. Future circular colliders. In *Future Research Infrastructures: Challenges and Opportunities*, pages 73–80. IOS Press, 2016.

[6] Michael Benedikt et al. FCC Integrated Programme Stage 1: The FCC-ee. 3 2025.

[7] K. Oide, M. Aiba, S. Aumon, M. Benedikt, A. Blondel, A. Bogomyagkov, M. Boscolo, H. Burkhardt, Y. Cai, A. Doblhammer, B. Haerer, B. Holzer, J. M. Jowett, I. Koop, M. Koratzinos, E. Levichev, L. Medina, K. Ohmi, Y. Papaphilippou, P. Piminov, D. Shatilov, S. Sinyatkin, M. Sullivan,

J. Wenninger, U. Wienands, D. Zhou, and F. Zimmermann. Design of beam optics for the future circular collider e^+e^- collider rings. *Phys. Rev. Accel. Beams*, 19:111005, Nov 2016.

[8] Pantaleo Raimondi and Simone Maria Liuzzo. Toward a diffraction limited light source. *Phys. Rev. Accel. Beams*, 26:021601, Feb 2023.

[9] BJ Holzer. Introduction to transverse beam dynamics. *arXiv preprint arXiv:1404.0923*, 2014.

[10] *Electromagnetic Fields in Accelerator Components*, chapter Chapter 1, pages 3–81.

[11] S. Russenschuck. Design of accelerator magnets. In *CERN Accelerator School: Introduction to Accelerator Physics*, pages 118–153, 10 2000.

[12] P. J. BRYANT. *BEAM OPTICS AND LATTICE DESIGN*, pages 31–66.

[13] Helmut Wiedemann. *Particle accelerator physics*. Springer Nature, 2015.

[14] Shyh-Yuan Lee. *Accelerator physics*. World Scientific Publishing Company, 2018.

[15] Ralph J Steinhagen. Tune and chromaticity diagnostics. 2009.

[16] Michiko G Minty and Frank Zimmermann. *Measurement and control of charged particle beams*. Springer Nature, 2003.

[17] Rhodri Jones. Measuring Tune, Chromaticity and Coupling. 5 2020.

[18] Giovanni Iadarola et al. Xsuite: An Integrated Beam Physics Simulation Framework. *JACoW*, HB2023:TUA2I1, 2024.

[19] Andy Langner, Jaime Maria Coello de Portugal, Piotr Skowroński, and Rogelio Tomás. Developments of the segment-by-segment technique for optics corrections in the lhc. Technical report, 2015.